Published as:

Brew, G. E., Litak, R. K., Seber, D., Barazangi, M., Sawaf, T., and Al-Imam, A., Basement depth and velocity structure in the northern Arabian platform, Eastern Syria, Geophys. J. Int., 128, 617-631, 1997.

Basement Depth and Sedimentary Velocity Structure in the Northern Arabian Platform, Eastern Syria

GRAHAM E. BREW, ROBERT K. LITAK, DOGAN SEBER, MUAWIA BARAZANGI

Institute for the Study of the Continents and the Department of Geological Sciences,

Snee Hall, Cornell University, Ithaca, New York 14853, USA

ANWAR AL-IMAM, TARIF SAWAF

Syrian Petroleum Company, Ministry of Petroleum and Mineral Resources, Damascus, Syria

Abbreviated Title: **Basement depth in eastern Syria**

SUMMARY

Basement depth in the Arabian plate beneath eastern Syria is found to be much deeper than previously supposed. Deep-seated faulting in the Euphrates fault system is also documented. Data from a detailed, 300 km long, reversed refraction profile, with offsets up to 54 km, are analyzed and interpreted, yielding a velocity model for the upper ~ 9 km of continental crust. The interpretation integrates the refraction data with seismic reflection profiles, well logs and potential field data,

such that the results are consistent with all available information. A model of sedimentary thicknesses and seismic velocities throughout the region is established. Basement depth on the north side of the Euphrates is interpreted to be around 6 km, whilst south of the Euphrates basement depth is at least 8.5 km. Consequently, the potentially hydrocarbon-rich pre-Mesozoic section is shown, in places, to be at least 7 km thick. The dramatic difference in basement depth on adjacent sides of the Euphrates graben system may suggest that the Euphrates system is a suture / shear zone, possibly inherited from Late Proterozoic accretion of the Arabian plate. Gravity modeling across the southeast Euphrates system tends to support this hypothesis. Incorporation of previous results allows us to establish the first-order trends in basement depth throughout Syria.

Keywords: *Syria; Middle East; Refraction; Basement; Euphrates; Geophysics*

INTRODUCTION AND GEOLOGIC BACKGROUND

We present an interpretation of seismic refraction data collected along a north-south profile in eastern Syria. The refraction data are interpreted in conjunction with well logs, seismic reflection data, gravity and magnetic data. Hence, previously unknown metamorphic basement depth, and pre-Mesozoic sedimentary thickness, in eastern Syria are established. Along with indications of basement and deep sedimentary structure, this can help to determine the intracontinental tectonic processes that have shaped the region.

The tectonic setting of Syria within the Arabian plate (Fig. 1) shows that the country is almost surrounded by active plate boundaries. The western boundary is marked by the left-lateral Dead Sea fault system which extends from the Gulf of Aqaba

in the south to the Cyprus subduction zone - Bitlis suture - Dead Sea transform triple junction in the north. The Dead Sea fault marks the boundary between the Arabian plate to the east and the Levantine (east Mediterranean) subplate to the west. To the north of Syria lies the Bitlis suture which represents the collision zone of the Arabian and Eurasian plates. Continuing movement along this boundary is accommodated by thrusting along the Bitlis suture as well as movement on the East Anatolian left-lateral fault, as the Anatolian subplate maneuvers to escape collision. To the east and southeast of Syria the Neogene-Quaternary Zagros fold belt marks the collision zone of the Arabian plate with Iran (e.g. Sengor & Kidd 1979; Sengor & Yilmaz 1981).

It is generally believed that the movement along the surrounding plate boundaries controls the intraplate deformation observed in Syria (e.g. Barazangi *et al.* 1993). The two main structural features of the country are the Palmyride fold and thrust belt of central Syria, and the Euphrates fault system in the east (Fig. 2). It has been suggested (e.g. Best *et al.* 1990) that these structures could be formed by reactivation along zones of weakness in the Arabian plate - weaknesses that have perhaps persisted since the Proterozoic (e.g. Barazangi *et al.* 1993; Litak *et al.* 1996a). However, whilst an appreciable amount of research has been conducted in the Palmyrides (e.g. Chaimov *et al*. 1990; McBride *et al*. 1990; Al-Saad *et al*. 1992; Barazangi *et al*. 1992), relatively little work has focused on eastern Syria. In particular, the Euphrates system has received limited attention in comparison to its geologic and economic importance (e.g. Beydoun 1991; de Ruiter *et al*. 1994). Recent work (Sawaf *et al*. 1993; Alsdorf *et al*. 1995; Litak *et al*. 1996a, 1996b) has increased understanding of the Euphrates system, but detailed assessment of basement structure and depth in this region has, until now, been unavailable. Hence, our results are a valuable contribution to the knowledge and understanding of the regional structure and tectonics of eastern Syria.

The area of eastern Syria focused upon in this study can be roughly divided into four structural zones of intraplate deformation, within which the deformation appears to

be controlled by movement on the nearby plate boundaries. From north to south these are the Abd el Aziz structural zone, the Derro high, the Euphrates fault system and the Rutbah uplift (Fig. 2).

The Abd el Aziz uplift is an anticlinorium controlled mainly by a major south-dipping reverse fault (e.g. Ponikarov 1967; Lovelock 1984). It is thought that the Abd el Aziz was a sedimentary basin in the Mesozoic which inverted in the Neogene (Sawaf *et al*. 1993), and may have been the northwestern edge of the larger Sinjar trough which existed at that time (Lovelock 1984).

South of Abd el Aziz, and to the north of the Euphrates, is a series of structural highs, controlled by deeply penetrating faults. Most prominent of these is the Derro high which is interpreted to be bounded by north-dipping reverse faults that separate this area from the Abd el Aziz (Sawaf *et al*. 1993). Basaltic outcrops along some of the larger faults around the Derro high could offer further evidence for the deep-seated nature of faulting in this area.

Although largely unexpressed by surface features, the Euphrates fault system represents an aborted rift system, striking roughly NW-SE and extending completely across Syria. The faulting is thought to represent a Late Cretaceous transtensional graben system with minor reactivation in Neogene times (Lovelock 1984). The system can be roughly divided into three parts along its length (Litak *et al*. 1996a): a northwestern segment exhibiting shallow grabens and significant inversion; a central segment where the Euphrates system bounds the Palmyrides and strike-slip movement is apparent; and the southeastern part which is characterized by deep graben features and only very minor inversion (Fig. 2). Although Lovelock (1984) suggested that most movement in the system took place on a few major faults, recent work clearly indicates that the deformation is widely distributed (de Ruiter *et al.* 1994; Litak *et al.* 1996a, 1996b). Faulting, for the most part, is nearly vertical in most places, resulting in limited (< 6 km) extension across the system (Litak *et al*. 1996b).

The southernmost section of the refraction profile crosses the eastern edge of the Rutbah uplift, an extensive upwarp which affects large parts of western Iraq, northern Jordan and southern Syria. Doming and extensive erosion of the area is known to have taken place during the Mesozoic and Tertiary (e.g. Lovelock 1984). Very little deformation is found in the strata of the Rutbah Uplift, except along the northeastern edge where it trends into the Euphrates depression.

Basement Rocks in Syria

The lack of current constraints on basement depth in Syria is a consequence of an almost complete absence of basement outcrops, and only one well, in the far northwest of the country, has penetrated the Precambrian (Ponikarov 1967). The few basement exposures that exist are in northwest Syria, Jordan, southern Israel and in southern Turkey, all at extensive distances from the study area, and in different geologic regimes (Ponikarov 1967; Sawaf *et al*. 1993). Leonov *et al*. (1989) constructed a depth to basement map within Syria based on well data and seismic reflection data, thus establishing the broad trends which are still generally accepted. However, the small scale and lack of direct evidence used in the study of Leonov *et al*. (1989) limit its applicability and new results presented here disagree somewhat with this earlier assessment. Best *et al.* (1993) mapped basement for the whole of Syria by using a prominent Mid-Cambrian reflection event as a proxy for basement rocks. However the results presented here show there can be substantial differences between the depth of the Middle Cambrian and basement rocks. Seber *et al*. (1993), using seismic refraction data, established basement depths in central Syria to be around 6 km beneath the Aleppo Plateau, 9-11 km beneath the Palmyrides and at least 8 km in the south of the country. Additionally, Seber *et al*. (1993) found seismic velocities of basement rocks to be around 6 km s^{-1}, in agreement with the findings of refraction surveys in Jordan which interpreted basement velocities of 5.8 - 6.5 km s^{-1} (Ginzburg *et al.* 1979; El-Isa *et al*. 1987). However, in the absence of

previous investigations in eastern Syria, the results presented here offer a unique assessment of basement depth in this region, and hence offer new insight on the deformational history of the northern Arabian platform.

DATA ANALYSIS

Data Acquisition

The model of basement depth and deep sedimentary structure that we develop relies on the analysis of several data sources, particularly a 300 km long seismic refraction profile. The refraction data were collected as part of a larger seismic profiling effort spanning all of Syria, conducted by a Soviet/Syrian joint project in 1972-3. Nine refraction lines were shot, totaling 2592 km, providing unique data for the study of deep sedimentary structure.

The original analysis of the seismic refraction data (Ouglanov *et al*. 1974) relied on interpretation techniques that established velocities using simplistic formulae that are now known to be problematic. Additionally, the original interpretation attached stratigraphic significance to some of the velocity contrasts observed in the refraction interpretation. Data from wells drilled since this initial interpretation show these stratigraphic inferences to be incorrect. However, as this old interpretation was never written in final form, and was never published, further results of the 1974 analysis of the data are not discussed here. With the benefit of technological advances in the interpretation of these type of data, and aided by extensive supplementary data sources, we present a new interpretation of the original data showing basement depth to be much greater than originally interpreted.

Fig. 2 shows the location of the refraction profile, the seismic reflection lines and the well logs used in this interpretation. The refraction line is 302 km long and oriented north-south. A total of 44 shot points were employed along the profile having a spacing of approximately 7 km. Shot sizes varied between 50 and 1250 kg dependent on geophone offset; data were recorded along forward and reverse geophone spreads for each shot, and geophone spacing was 150 meters. For most shots both a high and low gain analog recording were made. The geophone spreads were of two types: every second shot point had 'short' spreads of 28 km maximum offset and the remaining, 'long', spreads had nominal maximum offsets of 48 km, with the longest spread being 54 km.

Since deep sedimentary structure was the primary focus of this investigation, it was decided that the shorter spreads (28 km offsets) contained little data that could not be obtained independently from the longer spreads. Thus, data from 23 shots, each with forward and reverse geophone spreads, are used in our interpretation. This yields a fold of coverage at least 700% in most places (Fig. 3), unusually high for a survey of this type.

In analyzing these data the original photographic analog recordings from the survey were used to digitize first and, wherever possible, subsequent arrivals. Recognition of first arrivals was generally unambiguous owing to large shot sizes and relatively quiet recording conditions (Fig. 4). Identification of subsequent arrivals, however, was generally precluded by the large amplitudes of the traces and short recording times. A total of approximately 17,000 arrivals were digitized.

Data Interpretation

The refraction data were interpreted using a geometric ray-tracing approach utilizing the software of Luetgert (1992). Preliminary interpretation involved simple refraction modeling; the positions and velocities of various user-defined layers in the

software were subtly altered until travel times of calculated rays-paths through the computer model matched those of the digitized arrival times. This preliminary-type interpretation produced a 7 layer model with seismic velocity increasing in each deeper layer. Although naturally in agreement with the refraction data, the velocity interfaces in this model were found to be in disagreement with some velocity boundaries observed in sonic logs and travel times from seismic reflection data. The disagreement was largely a consequence of the limitations in the refraction method, in particular the inability to resolve low-velocity layers that are clearly demonstrated by the sonic logs (Fig. 5).

However_, the ambiguity of low-velocity layers can be eliminated if velocity information is available from an independent source, or if reflection travel times are known in addition to refraction times_ (e.g. Kaila, Tewari & Krishna 1981). Therefore, an interpretation strategy was adopted in which the refraction, reflection and well data were used simultaneously in the refinement of the velocity model, thus establishing a model consistent with all available data. This began with the construction of an initial velocity model constrained at shallow depths (< 4 km) by seismic reflection and well data, with sonic logs from parts of 3 wells (Fig. 2) allowing estimates of seismic velocities. The deeper section of the initial model was less constrained and relied on extrapolation from the shallow section and limited reflection data. The ground surface of the model was extracted from digital topographic data, sub-sampled to approximately 1 km horizontal resolution. The initial model was refined through ray-tracing to improve agreement with the various data, in particular the refraction arrival times. The modeling effort, described further below, culminated in what is hereafter referred to as the 'final velocity model' - a model consistent with all the available data.

Due to the high fold of coverage of the refraction data, and the various other constraining data, many iterations were necessary to produce a velocity model in agreement with all the data. The refraction interpretation was done by taking each individual shot in turn, and changing the velocity model to produce the best between the

observed and the calculated arrivals for that shot. However, due to the higher than 100% fold of coverage, modifications made to the model by examining the fit for one shot obviously changed the fit between the observed and calculated arrivals for other adjacent shots. Thus, after each change to the velocity model, the fit between the calculated and observed arrivals from every shot had to be checked. The final velocity model was determined by obtained the best overall fit of the arrivals for all the shots. Although this was extremely time-consuming, the process yielded an essentially unique velocity model that is in agreement with all the refraction arrivals.

It was clear from the integrated modeling that some of the velocity interfaces detected by the refraction data coincided with age horizons and associated velocity changes in sonic log data. Fig. 5 shows the sonic log and synthetic seismogram from the Derro well, along with velocities from the final velocity model. This shows how the velocities in the final model fit those found in the sonic log, whilst at the same time the depths of the velocity interfaces match the depths of certain age horizons found in the well. Where such correlations were observed the velocity model was modified to fit both the well data and the refraction data as accurately as possible.

Knowing the age of certain velocity interfaces, reflection data were utilized in conjunction with the refraction data. Two-way reflection times derived from the final velocity model and those from seismic reflection data were compared to support the refraction interpretation and add further detail which could not be resolved by the refraction method alone. For example, faults interpreted from seismic reflection data were used to refine the detail of the final velocity model (e.g. Fig. 6a). Fig. 6 shows examples of how two-way times in the final velocity model compare to those from seismic reflection data. Although not all prominent reflections are associated with refractions (e.g. mid-Cambrian reflector, Fig. 6b) most of the reflectors are correlated to refracting horizons, indicating a similar physical nature for refracting and reflecting horizons.

Aeromagnetic data (Filatov & Krasnov, 1959) show few anomalies of interest from the study region, with generally long wavelength, low amplitude variations indicating sources at significant depths. Assuming the source of the anomalies to be basement rocks then the magnetic data agree with the observations of large basement depths established in the velocity model, with shallower sources in the north. Isolated patches of short wavelength, high amplitude magnetic anomalies correspond with known basaltic outcrops. Additionally, gravity observations along the profile (BEICIP 1975) were compared to the gravity signature of the velocity model, with each velocity layer assigned an appropriate density. In this case also, the calculated and observed observations show overall agreement. More analysis of gravity data is presented in the next section.

The Final Velocity Model

The final velocity model that satisfactorily fits all available data is presented in Fig. 7a. The velocities in some of the layers change laterally, but layers have uniform velocities in a vertical direction. Well data along the profile, superimposed on the velocity interfaces and their presumed stratigraphic significance, demonstrate the close semblance between the model and well data (Fig. 7b).

However, despite direct evidence for the majority of the model, a few uncertainties remain. For example, no direct evidence exists for parts of some low velocity layers, hence the exact position of these horizons is, in places, uncertain. It is also not possible to obtain exact measures of the velocities of the low-velocity zones in these cases and so parts of the layers have been given velocities that are interpolations between well-determined values. Additionally, the depth to basement in the far south of the model is only thought to be a minimum constraint. No refractions were observed in this part of the refraction profile at velocities considered typical of those for metamorphic basement rocks, either because basement velocities are appreciably slower in this region, or

because the geophone spreads employed were too short to sample refractions from the apparently deeper basement in this region. The latter explanation is considered more probable, therefore the depth to basement shown is a minimum (Fig. 7). Another uncertainty concerns the interface signified as top of Khanasser (Lower Ordovician) in the north of the model. The interface interpreted based on the refraction data does not correspond exactly with observations from the Jafer well (Fig. 7b). Therefore, the refractor in this region is labeled 'Infra-Khanasser'.

Despite these shortcomings, the majority of the final velocity model is based on direct evidence from at least one and, in many cases, several sources. In general, the modeled refraction times show excellent agreement with the observed arrivals from the refraction data. Four examples of this, from various points in the transect, are shown in Figure 8. Each of the other shots, not shown here, demonstrate similar agreement between the velocity model and the observed arrival times. Given reasonable inaccuracies in the fit between observed and calculated refraction arrivals, such as those indicated in Figure 8, the errors in the bulk of the model can be shown to be relatively small, with approximately ± 200 m error in depth to most interfaces and less than ± 0.1 km s^{-1} in velocities.

DISCUSSION

A model of seismic velocity down to basement in eastern Syria has been constructed from the interpretation of refraction data and additional coincident data sources (Fig. 7). The model shows basement-involved tectonics beneath the Euphrates graben system and the Abd el Aziz uplift. The faulting is steeply dipping (even though the model is oblique to the dominant strike of the area), a result supported by the extensive seismic reflection analysis of Litak *et al*. (1996b). In the area where the

refraction transect crosses the Euphrates, Litak *et al*. (1996b) reported that the graben morphology in the upper sedimentary section is similar to the 'classic' model of a normally-faulted rift system, more so than elsewhere along the Euphrates. Our model shows this style of faulting persists to basement depth.

The model indicates that whilst increasing formation age generally causes increasing seismic velocity, velocity is also controlled by depth of burial and, more significantly, by lithology. These, and other ideas, are explored below as each of the velocity layers, from shallowest to deepest, are discussed in relation to their stratigraphic significance and relevance to regional tectonics.

Cenozoic and Mesozoic

The uppermost velocity layer (2.2 km s^{-1}), is interpreted as being a superficial covering of weathered and poorly consolidated material underlain by more competent rocks of various ages (3.2 - 3.6 km s^{-1}). Somewhat deeper is a relatively high velocity (4.7 km s^{-1}) layer extending across the middle portion of the model (Fig. 7a). This stratum hindered refraction interpretation by acting as a 'screening layer' (as described by Rosenbaum 1965; Poley and Nooteboom 1966), preventing some seismic energy from reaching deeper interfaces. However, enough energy was returned from deeper horizons to permit meaningful analysis (e.g. Fig. 8c). The position of the 4.7 km s^{-1} layer was correlated with well data (Figs 5 and 7b) to a Middle Miocene sequence of anhydrites, gypsum and limestone, known locally as the 'Transition Zone' (Sawaf *et al*. 1993). Slight doming of this horizon, as well as the underlying top of Cretaceous interface, that was not detected as a refractor but which is mapped on the basis of well logs and reflection data, may be due to minor inversion on the north side of the Euphrates graben. This inversion is probably the result of the continued Cenozoic collision between the Arabian and Eurasian plates along the Bitlis suture and Zagros collision zone (Litak *et al.* 1996b).

Below the Cretaceous, the Triassic layer (5.1 - 5.4 km/s), of predominantly dolomites and anhydrites, produces good refractions of characteristically high seismic velocity. The Triassic strata pinch out in the south whilst thinning slightly away from the graben toward the north (Fig. 7b).

Paleozoic

The Upper Paleozoic formations - Permian, Carboniferous, Silurian (Devonian is entirely absent) - are grouped together on the basis of their similar seismic velocities (3.2 - 3.6 km s^{-1}) (Fig. 7a). These mainly shale and sandy shale formations (Table 1), show slight thinning towards the north. The thinning is a result of extensive erosion that took place whilst northern Syria formed an intermittent broad subaerial uplift from Late Silurian to Permian time (Sawaf *et al.* 1993). The uppermost Ordovician, the Affendi formation (5.0 - 5.1 km s^{-1}), is clearly of higher velocity than the overlying rocks, presumably due to its predominately sandstone lithology. The Affendi formation shows thinning by around 2 km from south to north, again possibly due to uplift in northern Syria.

Below the Affendi formation is a 4.0 - 4.2 km s^{-1} layer corresponding to the shaley Swab formation of Early Ordovician age deposited during the Llandeilian regression (Husseini 1990). Beneath the Swab is the lowest Ordovician formation, the Khanasser, a predominately quartzitic sandstone unit with correspondingly high seismic velocity of 5.5 - 5.6 km s^{-1}. The Khanasser formation, combined with the Upper Cambrian sediments, show a thickening of around 1.7 km from south to north. This observation corresponds with the map of Husseini (1989) that shows isopachs of these units following the edge of the Arabian plate, with thickening of the Upper Cambrian/Lower Ordovician sediments away from the center of the Arabian platform towards the Tethys Ocean to the northeast.

Global sea-level rise in the Early to Mid-Cambrian caused the deposition of an extensive carbonate layer, the Mid-Cambrian Burj limestone, throughout Syria. Due to

the high impedance contrast with the surrounding clastic rocks, this horizon forms a prominent reflection event which is correlated across much of the country (e.g. Fig. 6b). However, perhaps because of the limited thickness of this unit (< 200 meters), no definitive refraction arrivals are observed from the Burj formation. Thus reflection times from seismic data have been combined with the velocity model to give an approximate position of the Burj limestone within the model (Fig. 7b).

Thinning of the strata between the Burj limestone and basement rocks by more than 2 km from the south to the north is observed (Fig. 7b). This extensive thickness of Lower Cambrian / Precambrian clastics to the south of the Euphrates could be a consequence of pre-Mid-Cambrian rifting and subsidence. It is thought that during the Early Cambrian (600 - 540 Ma) the Arabian plate underwent NW-SE crustal extension (e.g. Husseini 1988, 1989; Cater & Tunbridge 1992). This rifting is evidenced in the extensive evaporite basins of Pakistan, Oman and the Arabian Gulf region, and rifting farther to the northwest is possible.

Seber *et al.* (1993), using similar refraction data, also established a thickened pre-Mid- Cambrian section in south-central Syria, as did the gravity interpretation of Best *et al.* (1990) which showed the likelihood of thickened Lower Paleozoic / Precambrian sediments to the south of the Palmyrides. These observations could show that the Early Cambrian rifting was extensive across southern Syria whilst the north of the country remained structurally high.

An alternative, better supported, explanation for the thickened pre-Mid-Cambrian section in the south, could be that the Euphrates trend formed a suture / shear zone caused by the Proterozoic accretion of the Arabian plate. This idea is expanded upon in the Precambrian discussion below.

Overall, the thickness of the pre-Mesozoic sedimentary section demonstrated here is significantly greater, by more than 3 km in places, than any previous estimates. These observations have important economic implications since extensive Paleozoic clastic

reservoir rocks and source rocks are known to exist in eastern Syria and elsewhere in the Middle East (e.g. Husseini 1990). As emphasized in the regional summary of Beydoun (1991), Paleozoic plays are likely to be a significant factor in future Middle East hydrocarbon production.

Precambrian

Although no wells penetrate basement rocks in Syria and basement has not been unambiguously identified on seismic reflection sections, previous refraction studies (Ginzburg *et al.* 1979; El-Isa *et al*. 1987; Seber *et al*. 1993) have established basement velocities to be around 6 km s^{-1}. Therefore, we assume the velocity layer of 6 km s^{-1} in the velocity model represents basement (Fig. 7a). Across the Rutbah uplift in the far south of the profile, basement depth is at least 8.5 km. Along the southern margin of the Euphrates fault system we have definitive refraction arrivals that put the basement at 8 km below surface. North of this region, the basement deepens through faulting into the deepest part of the Euphrates graben system, where basement depth is around 9 km. To the north of the Euphrates basement depth is around 6 km.

Although previous investigations are consistent with these general trends in basement depth (Lovelock 1984; Leonov *et al*. 1989; Best *et al*. 1993), our interpretation generally puts basement somewhat deeper than the earlier suggestions. This is particularly true in the Rutbah uplift where the estimates of both Lovelock (1984) and Leonov *et al*. (1989) suggest basement depth at least 3 km shallower than the new results.

The obvious difference in basement depth on either side of the Euphrates graben system could be evidence of a terrane boundary along the Euphrates trend. The Arabian shield (Fig. 1) accreted from discrete crustal blocks during the Late Proterozoic (e.g. Fleck *et al*. 1980; Pallister *et al*. 1987; Stoesser & Camp 1985; Vail 1985) and it is thought that similar processes might have formed the northern Arabian platform. Zones of weakness inherited from the accretion might control regional tectonics in the platform

(e.g. Barazangi *et al.* 1993; Best *et al.* 1993, Litak *et al.* 1996a), but thick sedimentary cover across the region makes such ideas difficult to prove. The stark difference in basement depth across the Euphrates could be an indication of two different crustal blocks accreting somewhat to the southwest of what is now the Euphrates graben system. This accretion could have been in the form of a suture zone, a shear zone, or some combination of the two - current data do not allow the definition of the precise mechanism. The possible accretion event in Syria would have to be Proterozoic, or very early Phanerozoic, in age since seismic reflections from the Mid-Cambrian Burj limestone (e.g. Fig. 6b) are continuous across most of Syria (e.g. Best *et al*. 1993).

This accretionary hypothesis, previously implied by Best *et al*. (1993) and Sawaf *et al*. (1993), is also consistent with gravity investigations. Bouguer gravity observations (BEICIP 1975) show a clear difference across the Euphrates with generally high gravity values to the northeast, and lower values to the southwest of the graben system (Fig. 9a). We model a profile across these observations, constraining the upper structure of the model in accordance with seismic reflection interpretation, and changing the deep crustal structure to obtain the best fit with the gravity values. Densities are constrained in the upper section by well logs from the El Madabe and Thayyem wells (Fig. 2).

Fig. 9(b) shows a geological model that accounts for the gross trends in the gravity observations. The difference in gravity values on either side of the Euphrates is modeled by invoking differences in the density of basement and lower crustal rocks, and by differences in basement depth (as derived from our refraction modeling). Even though maximum basement depth to the southwest is largely unconstrained, modeling the large scale gravity anomaly with variations in basement depth alone is not plausible, and a crustal density contrast is required. In this model (Fig 9b) the difference in crustal density and basement depth on opposite sides of the Euphrates supports the suture / shear zone hypothesis. Previous gravity models (e.g. Best, Wilburt & Watkins 1973; Gibb & Thomas 1976) show that, in a wide variety of settings, crustal density contrasts are a

common feature of suture zones. The Euphrates graben is in isostatic equilibrium, compensated by an elevated Moho. It is interesting to note that the gravity observations also tend to refute the Early Cambrian / Late Proterozoic rifting hypothesis discussed in the previous section. The gravity observations do not support a thinning of the crust to the south, which one would expect in a rifted area.

Further gravity modeling (Fig. 9c) attempts to explain the local gravity high on the southwest margin of the Euphrates (labeled 'A' in Fig. 9a), which extends a considerable distance into Iraq to the southeast (not shown). Although a basement high is thought to exist in this area (based on seismic reflections from the Mid-Cambrian Burj reflector), no reasonable uplift of the basement could account for this significant gravity anomaly. The high could be explained by a dipping, high-density mafic body extending to Moho depth (Fig. 9c). The location of this gravity high also appears to correspond with a magnetic anomaly from a deep source, perhaps further evidence for a mafic or ultramafic body at depth within the crust. The dip of the body shown in Fig. 9c is fairly arbitrary, and many variations of this shape could be made to fit the observations. A similar high-density body was modeled by Hutchinson, Grow & Klitgord (1983) as part of their gravity interpretation of the Piedmont gravity gradient along a possible Appalachian suture zone.

Obviously, the gravity models presented here are highly non-unique (e.g. Hutchinson *et al.* 1983). Constant ambiguity exists between density and structure, for example, basement depth verses crustal density contrast. However, our gravity modeling appears to show that the hypothetical suture / shear zone across the Euphrates shares many features in common with other sutures documented elsewhere. Such a zone along the trend of the Euphrates graben could offer a unified explanation for various tectonic and geophysical observations in the area. The accretionary hypothesis lends considerable support to the ideas of Best *et al.* (1990, 1993) which were expanded upon by Litak *et al.* (1996a). These authors implied a regional NW-SE trend of weak zones beneath the

northern Arabian platform, inherited from Proterozoic / Earliest Phanerozoic tectonics, amongst which is the Euphrates trend.

Incorporation of our results with those from other workers leads to a regional picture of basement depth and trends across much of Syria. Fig. 10 shows our results, along with basement depths derived using similar data by Seber *et al*. (1993), and selected deep well data. We see a clear trend of deeper basement to the south of the Palmyrides and to the southwest of the Euphrates, and shallower basement to the north. The deepest basement is located actually beneath the Euphrates and Palmyride structures. The locations of possible suture / shear zones (modified from Best *et al.* 1993) are also shown. Whilst the suture / shear zones along the Euphrates and Palmyride trends have now been documented with gravity and refraction data, the zone to the northeast remains untested and is largely hypothetical.

CONCLUSIONS

Basement depth and the location of several deep sedimentary interfaces are mapped from the interpretation of seismic refraction data incorporated with seismic reflection data, well logs and potential field data. Thus, basement depth beneath eastern Syria is found to be greater, by between 1 and 3 km, than previously supposed. Across the Rutbah uplift the basement is at least 8.5 km deep, in the Euphrates depression it is around 9 km, and to the north of the Euphrates basement is between 5.5 and 6.5 km in depth (Fig. 7). Hence, extensive thicknesses of pre-Mesozoic rocks are documented. Deeply penetrating faults are identified in the Euphrates graben system demonstrating the thick-skinned tectonic style of this region. Incorporation of results from previous research allows gross trends in basement depth across Syria to be presented (Fig. 10).

Clearly different basement depths on the northern and southern sides of the Euphrates graben could be evidence for the Late Proterozoic accretion of the northern Arabian platform with the Euphrates fault system as a suture / shear zone. This idea is supported by gravity observations that suggest higher density crust to the northeast of the Euphrates trend - a common feature of other suture zones. This leads support to the speculation of a system of weak zones beneath the northern Arabian platform, inherited from Late Proterozoic / Early Cambrian accretion, which continue to control regional tectonics.

ACKNOWLEDGMENTS

The data for this study were provided by the Syrian Petroleum Company. This research was supported by Arco, Exxon, Mobil and Unocal. Partial support was also sponsored by the U.S. Department of Energy Contract #F19628-95-C-0092. We thank A. Calvert, F. Gomez, E. Sandvol and W. Beauchamp, all of Cornell University, for their useful comments and suggestions. We would also like to thank Alan Beck and one anonymous reviewer for their comments which helped to improve the paper. Institute for the Study of the Continents contribution number 231.

REFERENCES

Al-Saad, D., Sawaf, T., Gebran, A., Barazangi, M., Best, J. & Chaimov, T., 1992. Crustal structure of central Syria: the intracontinental Palmyride Mountain belt, *Tectonophysics*, **207**, 345-358.

Alsdorf, D., Barazangi, M., Litak, R., Seber, D., Sawaf, T. & Al-Saad, D., 1995. The intraplate Euphrates depression-Palmyrides mountain belt junction and relationship to Arabian plate boundary tectonics, *Annali Di Geofisica*, **38**, 385-397.

Barazangi, M., Seber, D., Al-Saad, D. & Sawaf, T., 1992. Structure of the intracontinental Palmyride mountain belt in Syria and its relationship to nearby Arabian plate boundaries, *Bulletin of Earth Sciences, Cukurova University, Adana, Turkey*, **20**, 111-118.

Barazangi, M., Seber, D., Chaimov, T., Best, J., Litak, R., Al-Saad, D. & Sawaf, T., 1993. Tectonic evolution of the northern Arabian plate in western Syria. In *Recent evolution and Seismicity of the Mediterranean Region*, edited by E. Boschi *et al*, 117-140. Netherlands: Kluwer Academic Publishers.

BEICIP, 1975. *Gravity maps of Syria: Damascus (Syria)*, Bur. Etud. Ind. Coop. Inst. Fr. Pet., Hauts de Seine, 96 pp.

Best, J. A., Barazangi, M., Al-Saad, D., Sawaf, T. & Gebran, A., 1990. Bouguer gravity trends and crustal structure of the Palmyride Mountain belt and surrounding northern Arabian platform in Syria, *Geology*, **18**, 1235-1239.

Best, J. A., Barazangi, M., Al-Saad, D., Sawaf, T. & Gebran, A., 1993. Continental margin evolution of the northern Arabian platform in Syria, *Am. Assoc. Petrol. Geol. Bull.*, **77**, 173-193.

Beydoun, Z. R., 1991. Arabian plate hydrocarbon geology and potential – a plate tectonic approach:. In *Studies in Geology*, **77**. Tulsa, Oklahoma, USA: American Association of Petroleum Geologists.

Cater, J. M. L. & Tunbridge, I. P., 1992. Paleozoic tectonic history of SE Turkey, *J. Petrol. Geol.*, **15**, 35-50.

Chaimov, T., Barazangi, M., Al-Saad, D., Sawaf, T. & Gebran, A., 1990. Crustal shortening in the Palmyride fold belt, Syria, and implications for movement along the Dead Sea fault system, *Tectonics,* **9**, 1369-1386.

de Ruiter, R. S. C., Lovelock, P. E. R. & Nabulsi, N., 1994. The Euphrates graben, Eastern Syria: A new petroleum province in the northern Middle East. In *Geo '94, Middle East Petroleum Geosciences*, edited by Moujahed Al-Husseini, 357-368. Manama, Bahrain: Gulf PetroLink.

El-Isa, Z., Mechie, J., Prodehl, C., Makris, J. & Rihm, R., 1987. A crustal structure study of Jordan derived from seismic refraction data, *Tectonophysics*, **138**, 235-253.

Filatov, V. & Krasnov, A., 1959. *On aeromagnetic surveys carried out over the Syrian territory, the United Arab Republic during 1958-1959*, (Unpublished), Technoexport, Damascus, 33 pp.

Fleck, R. J., Greenwood, W. R., Hadley, D. G., Anderson, R. E. & Schmidt, D. L., 1980. Rubidium-Strontium geochronology and plate-tectonic evolution of the southern part of the Arabian shield, *US Geol. Sur. Professional Paper,* **1131**, 38 pp.

Gibb, R. A. & Thomas, M. D., 1976. Gravity signature of fossil plate boundaries in the Canadian shield, *Nature*, **262**, 199-200.

Ginzburg, A., Markris, J., Fuchs, K., Prodehl, C., Kaminski, W., & Amitai, U., 1979. A seismic study of the crust and upper mantle of the Jordan-Dead Sea rift and their transition toward the Mediterranean Sea, *J. geophys. Res.*, **84**, 1569-1582.

Hutchinson, D. R., Grow, J. A. & Klitgord, K. D., 1983. Crustal structure beneath the southern Appalachians: nonuniqueness of gravity modeling. *Geology*, **11**, 611-615.

Husseini, M., 1988. The Arabian Infracambrian extensional system, *Tectonophysics*, **148**, 93-103.

Husseini, M. I., 1989. Tectonic and deposition model of late Precambrian-Cambrian Arabian and adjoining plates, *Am. Assoc. Petrol. Geol. Bull.*, **73**, 1117-1131.

Husseini, M. I., 1990. The Cambro-Ordovician Arabian and adjoining plates: A glacio-eustatic model, *J. Petrol. Geol.*, **13**, 276-288.

Kaila, K. L., Tewari, H. C. & Krishna, 1981. An indirect method for determining the thickness of a low-velocity layer underlying a high velocity layer, *Geophysics*, **46**, 1003-1008.

Leonov, Y. G., Sigachev, S. P., Otri, M., Yusef, A., Zaza, T. & Sawaf, T., 1989. New data on the Paleozoic complex of the platform cover of Syria, *Geotectonics*, **23**, 538-542.

Litak, R. K., Barazangi, M., Beauchamp, W., Seber, D., Brew, G., Sawaf, T & Al-Youssef, W., 1996a. Mesozoic-Cenozoic Evolution of the Euphrates Fault System, Syria: Implications for Regional Kinematics, Submitted to *Geol. Soc. Lon. J.*

Litak, R. K., Barazangi, M., Brew, G., Sawaf, T., Al-Imam, A. & Al-Youssef, W., 1996b. Structure and Evolution of the Petroliferous Euphrates Graben System, Southeast Syria, Submitted to *Am. Assoc. Petrol. Geol. Bull.*.

Lovelock, P. E. R., 1984. A review of the tectonics of the northern Middle East region, *Geol. Mag.*, **121**, 577-587.

Luetgert, J. H., 1992. Interactive two-dimensional seismic ray-tracing for the Macintosh™, *US Geol. Sur., Open File Report 92-356*, Menlo Park, California

McBride, J. H., Barazangi, M., Best, J., Al-Saad, D., Sawaf, T., Al-Otri, M. & Gebran, A., 1990. Seismic reflection structure of intracratonic Palmyride fold-thrust belt and surrounding Arabian platform, Syria, *Am. Assoc. Petrol. Geol. Bull.*, **74**, 238-259.

Ouglanov, V., Tatlybayev, M. & Nutrobkin, V., 1974. *Report on seismic profiling in the Syrian Arab Republic*, (Unpublished), General Petroleum Company Report, Aleppo, Syria, 73 pp.

Pallister, J. S., Stacey, J. S., Fischer, L. B. & Premo, W. R., 1987. Arabian shield ophiolites and late Proterozoic microplate accretion, *Geology*, **15**, 320-323.

Poley, J. Ph. & Nooteboom, 1966. Seismic refraction and screening by thin high-velocity layers (A scale model study). *Geophys. Prosp.*, **XIV**, 184-203.

Ponikarov, V. P., 1967. *The geology of Syria: explanatory notes on the geological map of Syria, scale 1:500,000 part I: stratigraphy, igneous rocks and tectonics*, Damascus, Syrian Arab Republic, Ministry of Industry.

Rosenbaum, J. H., 1965, Refraction arrivals through thin high-velocity layers. *Geophysics*, **30**, 204-212

Sawaf, T., Al-Saad, D., Gebran, A., Barazangi, M., Best, J. A. & Chaimov, T., 1993. Structure and stratigraphy of eastern Syria across the Euphrates depression, *Tectonophysics*, **220**, 267-281.

Seber, D., Barazangi, M., Chaimov, T., Al-Saad, D., Sawaf, T. & Khaddour, M., 1993. Upper crustal velocity structure and basement morphology beneath the intracontinental Palmyride fold-thrust belt and north Arabian platform in Syria, *Geophys. J. Int.*, **113**, 752-766.

Sengor, A. M. C. & Kidd, W. S. F., 1979. Post-collisional tectonics of the Turkish-Iranian plateau and a comparison with Tibet, *Tectonophysics*, **55**, 361-376.

Sengor, A. M. C. & Yilmaz, Y., 1981. Tethyan evolution of Turkey: A Plate tectonic approach, *Tectonophysics*, **75**, 181-241.

Stoesser, D. B. & Camp, V. E., 1985. Pan-African microplate accretion of the Arabian shield, *Geol. Soc. Am. Bull.*, **96**, 817-826.

Vail, J. R., 1985. Pan-African (late Precambrian) tectonic terrains and the reconstruction of the Arabian-Nubian Shield, *Geology*, **13**, 839-842.

FIGURE CAPTIONS

Table 1: Stratigraphy of the Paleozoic in Syria (modified from Best *et al.* 1993).

SYSTEM		**FORMATION**	**LITHOLOGY**
Permian		Amanous	Shale / sandstone
Carboniferous		Markada	Sandy shales
Devonian		-	(not present)
Silurian	Upper	-	(not present)
	Lower	Tanf	Shale
Ordovician	Upper	Affendi	Sandstone with minor shale
	Lower	Swab	Mainly shale
		Khanasser	Quartzitic sandstone
Cambrian		Sosink	Quartzitic sandstone
		Burj	Limestone
		Zabuk	Sandstone
Pre-Cambrian		Saramuj	?

Figure 1: Regional tectonic setting of the northern Arabian platform.

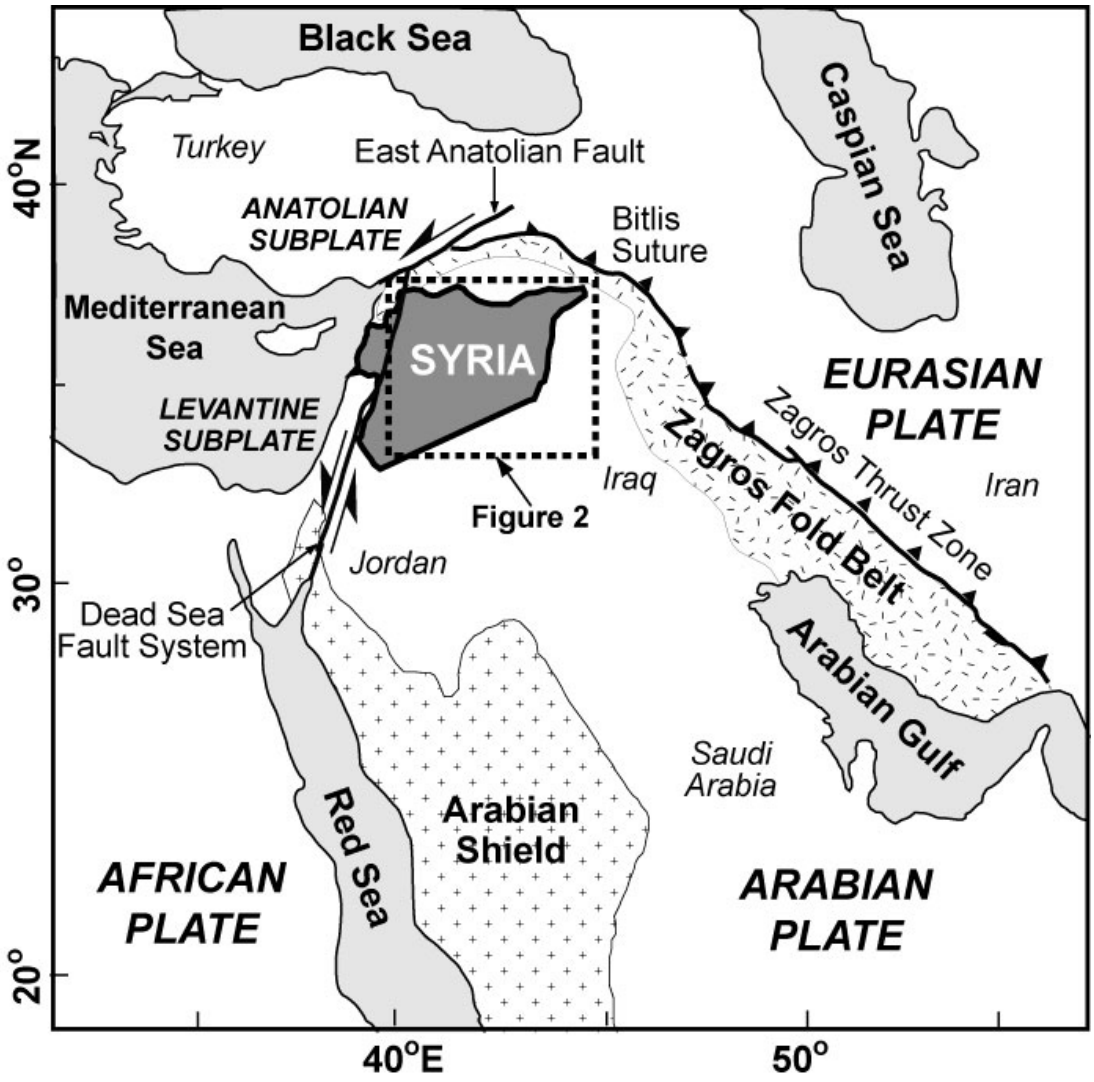

Figure 2: Map of eastern and central Syria showing location of selected data sources. Shaded area represents approximate location of Euphrates fault system. The extent of the faulting to the north and into Turkey is largely unconstrained. Only a small portion of the total number of seismic reflection lines used in this study are shown. Substantial additional well data farther from the refraction line were also available.

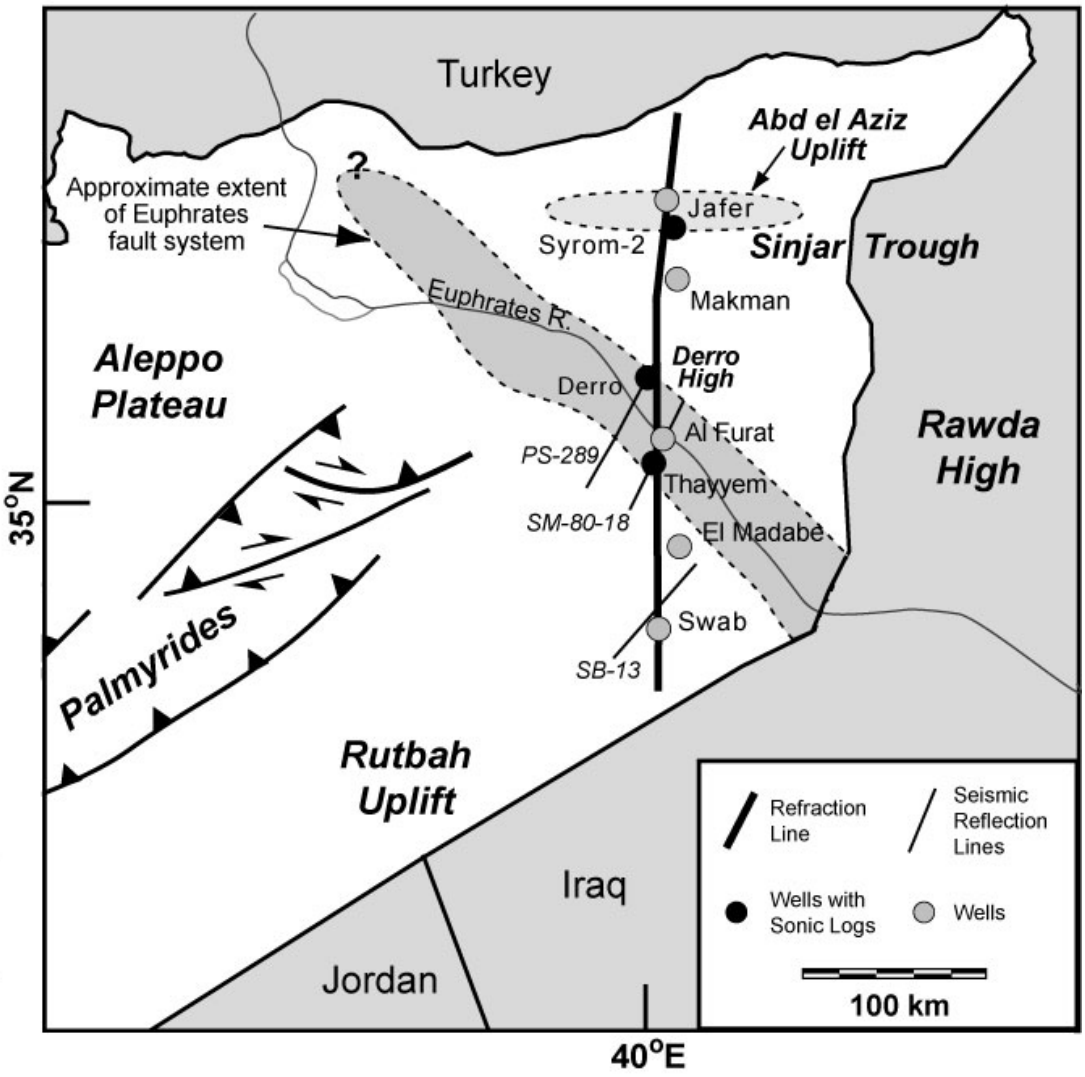

Figure 3: Configuration of shots and geophone spreads used in the refraction interpretation. Cumulative fold of coverage also shown.

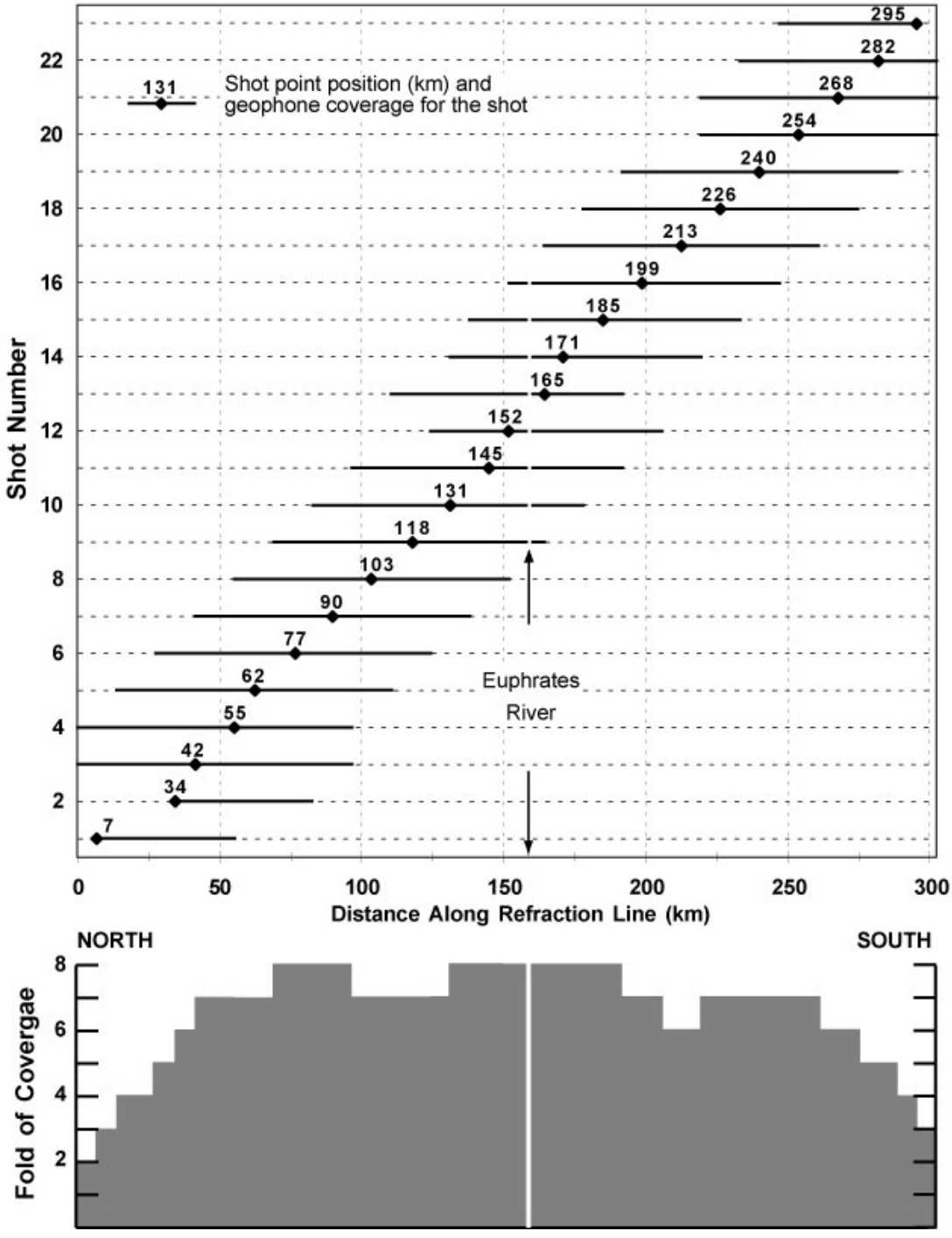
Shot point position (km) and
geophone coverage for the shot
Euphrates
River
Shot Number
Distance Along Refraction Line (km)
NORTH
SOUTH
Fold of Covergae

Figure 4: Typical example of original refraction data. Part of reverse spread from shot 17. Note the good quality of first arrivals (highlighted with line added by authors) which were digitized to accomplish a ray-traced interpretation.

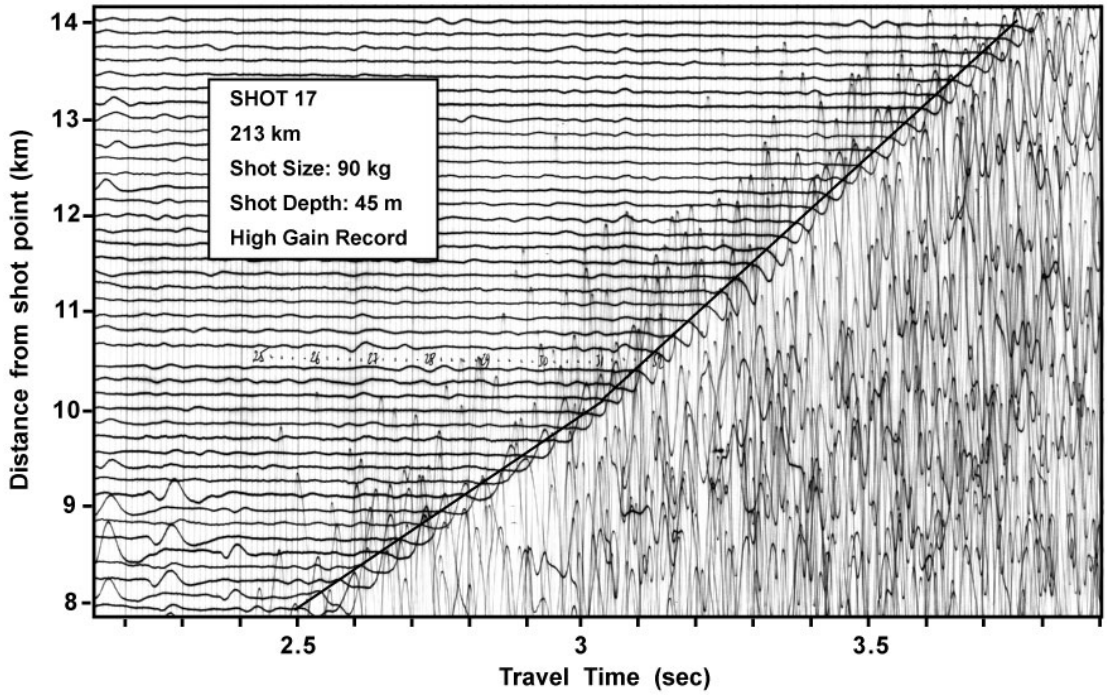

Figure 5: Sonic log and synthetic seismogram from Derro well (see Fig. 2 for location). Velocities from final velocity model shown by heavy gray line on same scale. Sonic logs from this and several other wells were used to constrain the velocity model. Note the low-velocity Upper Paleozoic strata which are undetectable by refraction data alone. Seismic line PS-289 at the tie with the Derro well is shown for comparison to the synthetic seismogram.

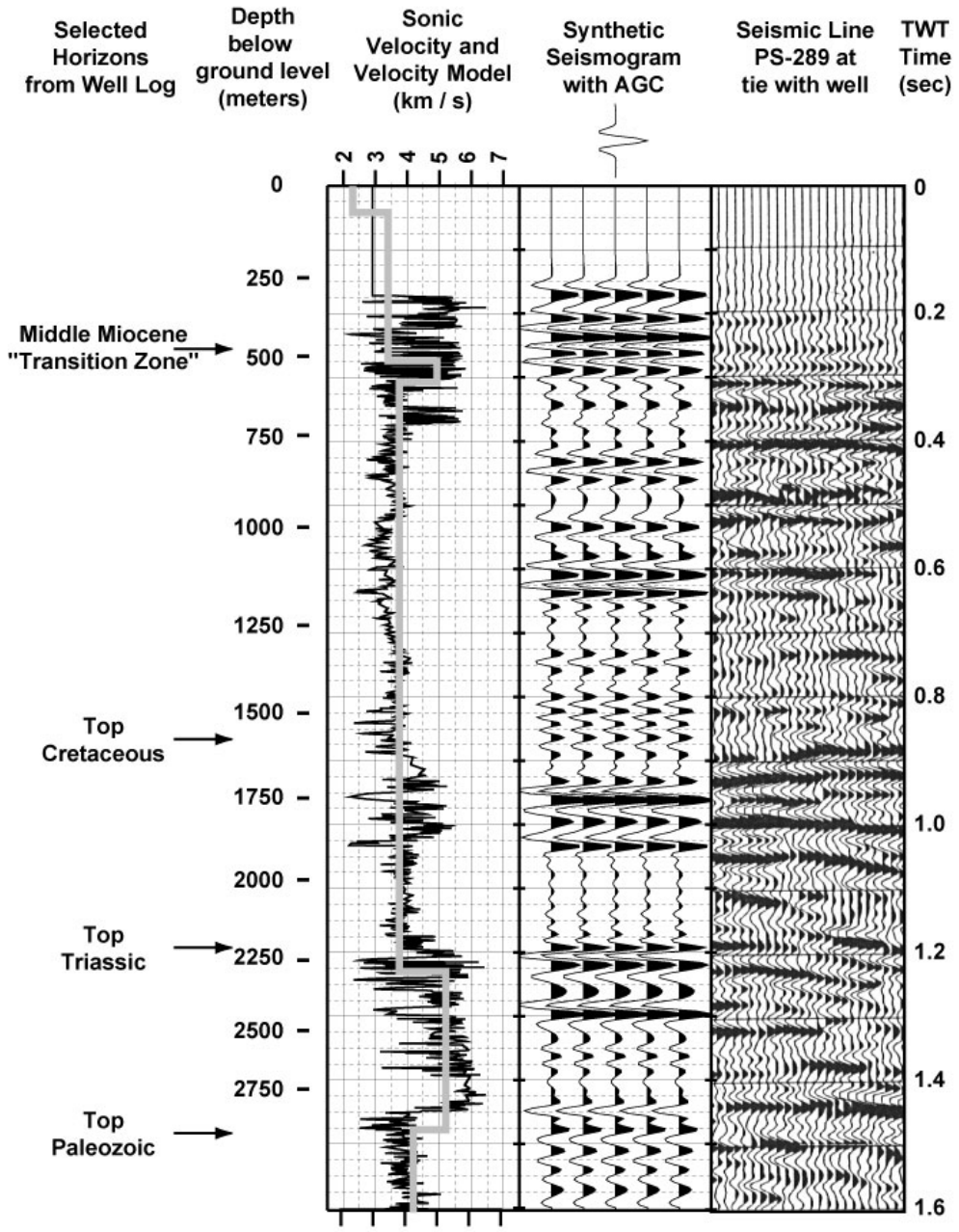
Selected Horizons from Well Log
Depth below ground level (meters)
Sonic Velocity and Velocity Model (km / s)
Synthetic Seismogram with AGC
Seismic Line PS-289 at tie with well
TWT Time (sec)
2
3
4
5
6
7
0
250
500
750
1000
1250
1500
1750
2000
2250
2500
2750
0
0.2
0.4
0.6
0.8
1.0
1.2
1.4
1.6
Middle Miocene "Transition Zone"
Top Cretaceous
Top Triassic
Top Paleozoic

Figure 6 (a, b): Examples of correlations between seismic reflection data and two-way incidence reflection times deduced from the velocity model (see Fig. 2 for location of seismic reflection lines). Interfaces not corresponding to velocity changes are shown as dotted lines on the velocity graph. Uncertain velocity interface positions shown as long dashed lines.

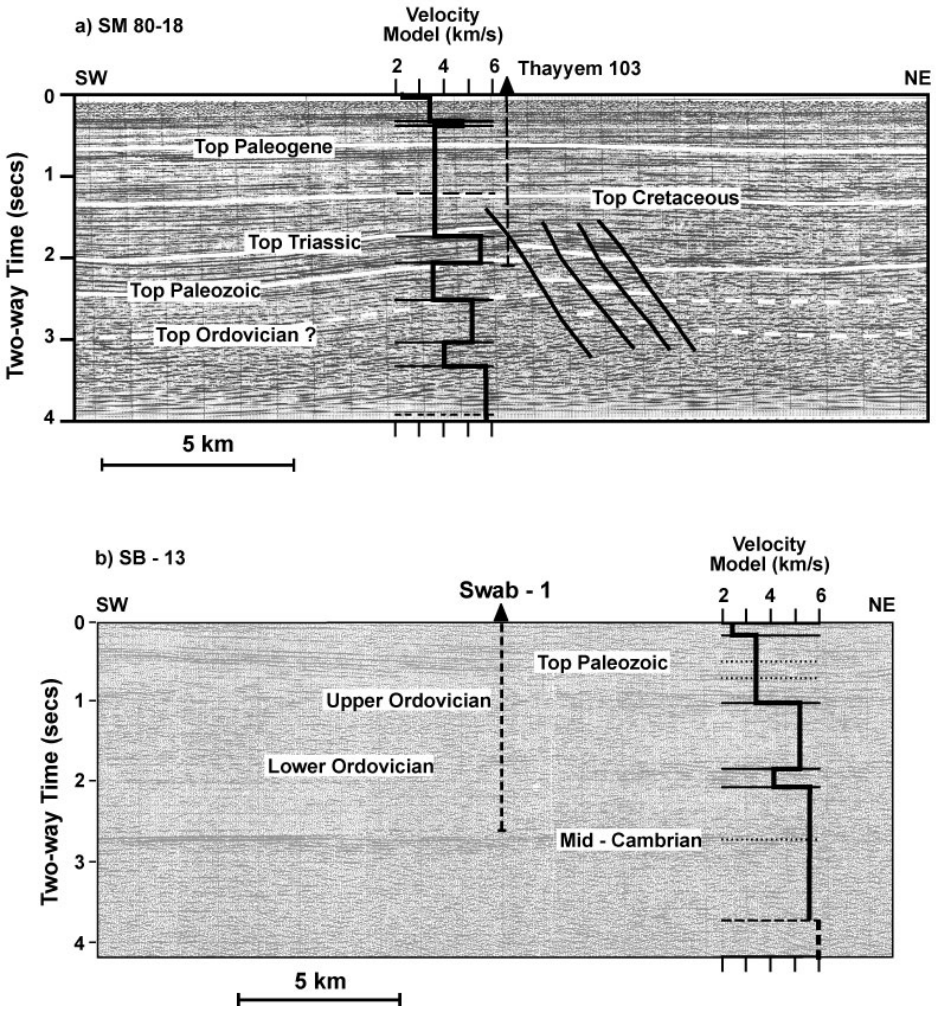

Figure 7: Cross section showing the final velocity model. Model interfaces not corresponding to velocity changes are shown as dotted lines. Uncertain interfaces positions shown as long dashed lines. (a) shows seismic velocity model and interface positions. Locations of shots used in Fig. 8 also shown. (b) demonstrates the correlation

between the velocity interfaces and age boundaries sampled in wells along the refraction profile.

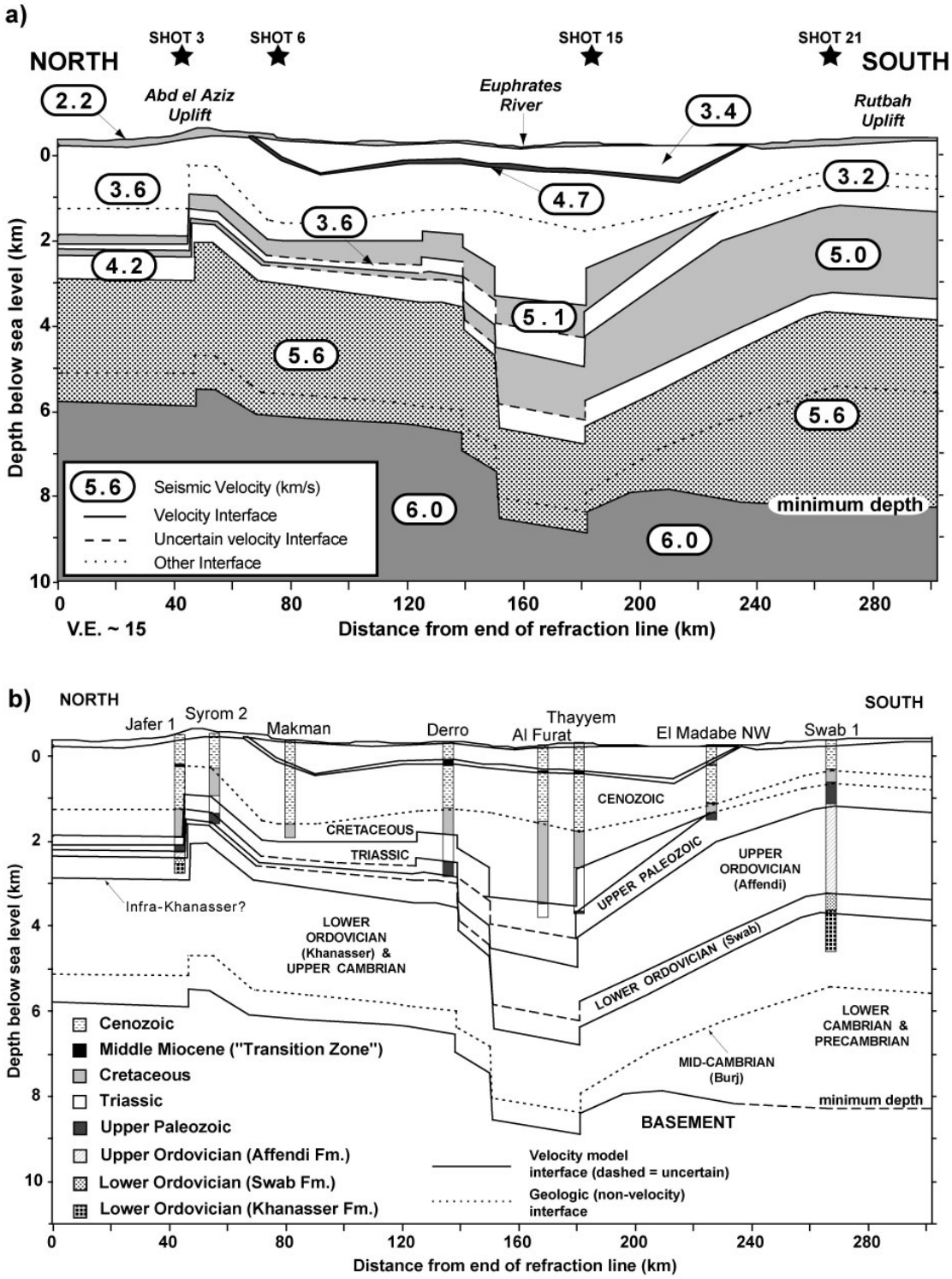

Figure 8 (a-d): Examples of ray-tracings from the final velocity model chosen to represent the full range of structures interpreted along the transect. Numbers represent

seismic velocities in km s^{-1}. Note the effect of the near-surface high-velocity layer in (c). Modeled refractions from basement in (d) do not necessarily fit observed arrivals, but are shown to illustrate that basement depth for this part of the model is a minimum.

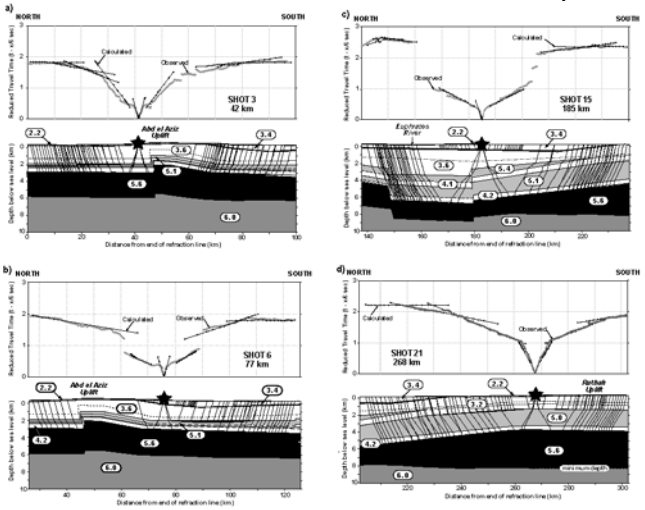

Figure 9: (a) Map showing Bouguer gravity anomalies in southeastern Syria across the Euphrates graben system. Bouguer reduction density = 2.53 kg m^{-3}. Contour interval 2 mGal. (b) Gravity model to explain gross trends in gravity anomalies. Gravity high to NE of Euphrates modeled using shallower basement and a reduction in crustal / upper mantle density contrast. (c) Refinement of the model in which gravity high 'A' in (a) is modeled with dipping high-density body in crust.

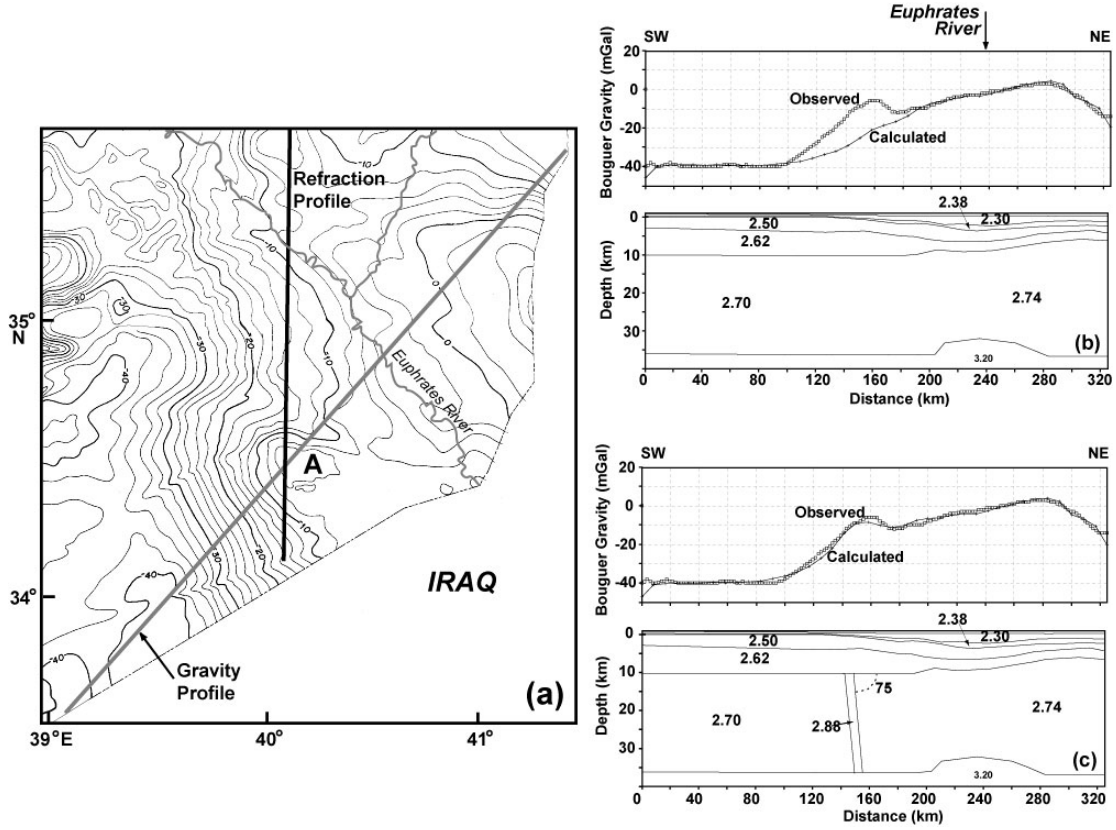
Refraction Profile
Euphrates River
A
IRAQ
Gravity Profile
(a)
35° N
34°
39°E
40°
41°
Euphrates River
SW
NE
Bouguer Gravity (mGal)
Observed
Calculated
Depth (km)
2.38
2.30
2.50
2.62
2.70
2.74
3.20
(b)
Distance (km)
75
2.88
(c)

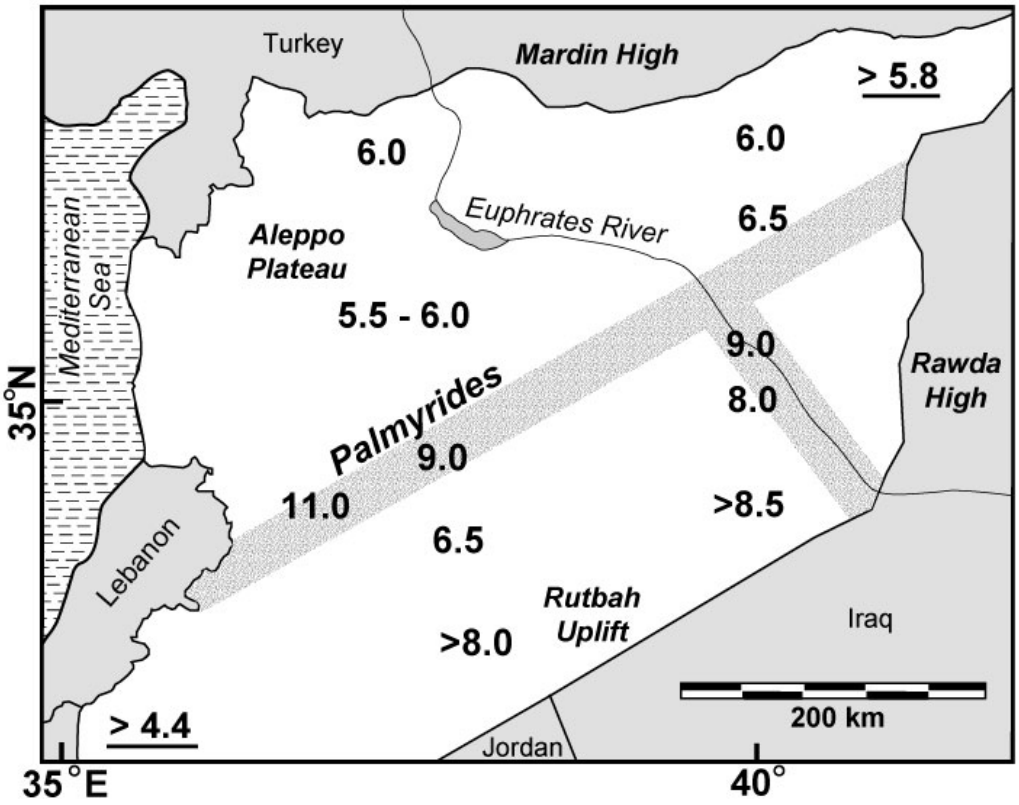

Figure 10: Map showing basement depths in Syria in kilometers below surface. Results from this study and previous refraction interpretation of Seber *et al*. (1993). Underlined data points are from selected deep well data. Shading represents locations of possible suture / shear zones.